Faculty Publications, Chemistry   Chemistry

1-1-2004

Lanthanide Spectroscopic Studies of the Dinuclear and Mg(II)-Dependent PvuII Restriction Endonuclease

Gilles Muller
San Jose State University, gilles.muller@sjsu.edu

L. M. Bowen
University of Missouri - St Louis

J. P. Riehl
University of Minnesota - Duluth

C. M. Dupureur
University of Missouri - St Louis

Follow this and additional works at: https://scholarworks.sjsu.edu/chem_pub

Part of the Chemistry Commons

Recommended Citation

Lanthanide Spectroscopic Studies of the Dinuclear and Mg(II)-Dependent *Pvu*II Restriction Endonuclease[†]

Lori M. Bowen,[‡] Gilles Muller,[§,||] James P. Riehl,[§] and Cynthia M. Dupureur*,[‡]

Department of Chemistry and Biochemistry, University of Missouri St. Louis, St. Louis, Missouri 63121, and Department of Chemistry, University of Minnesota Duluth, Duluth, Minnesota 55812

ABSTRACT: Type II restriction enzymes are homodimeric systems that bind four to eight base pair palindromic recognition sequences of DNA and catalyze metal ion-dependent phosphodiester cleavage. While Mg(II) is required for cleavage in these enzymes, in some systems Ca(II) promotes avid substrate binding and sequence discrimination. These properties make them useful model systems for understanding the roles of alkaline earth metal ions in nucleic acid processing. We have previously shown that two Ca(II) ions stimulate DNA binding by *Pvu*II endonuclease and that the trivalent lanthanide ions Tb(III) and Eu(III) support subnanomolar DNA binding in this system. Here we capitalize on this behavior, employing a unique combination of luminescence spectroscopy and DNA binding assays to characterize Ln(III) binding behavior by this enzyme. Upon excitation of tyrosine residues, the emissions of both Tb(III) and Eu(III) are enhanced severalfold. This enhancement is reduced by the addition of a large excess of Ca(II), indicating that these ions bind in the active site. Poor enhancements and affinities in the presence of the active site variant E68A indicate that Glu68 is an important Ln(III) ligand, similar to that observed with Ca(II), Mg(II), and Mn(II). At low micromolar Eu(III) concentrations in the presence of enzyme (10−20 μM), Eu(III) excitation $^7F_0 \rightarrow {}^5D_0$ spectra yield one dominant peak at 579.2 nm. A second, smaller peak at 579.4 nm is apparent at high Eu(III) concentrations (150 μM). Titration data for both Tb(III) and Eu(III) fit well to a two-site model featuring a strong site ($K_d = 1-3\ \mu$M) and a much weaker site ($K_d \approx 100-200\ \mu$M). Experiments with the E68A variant indicate that the Glu68 side chain is not required for the binding of this second Ln(III) equivalent; however, the dramatic increase in DNA binding affinity around 100 μM Ln(III) for the wild-type enzyme and metal-enhanced substrate affinity for E68A are consistent with functional relevance for this weaker site. This discrimination of sites should make it possible to use lanthanide substitution and lanthanide spectroscopy to probe individual metal ion binding sites, thus adding an important tool to the study of restriction enzyme structure and function.

The alkaline earth divalent cations Mg(II) and Ca(II) are important to many biological processes. Present in high concentrations in cells, Ca(II) is involved in signaling cascades, enzyme activation, and muscle contraction. Mg(II) plays vital roles in enzyme activation and nucleic acid stabilization (*1*). The properties of Mg(II) and Ca(II), in particular the preference for oxygen ligands, make them natural cofactors in the processing of nucleic acids. They are required in a number of well-known nuclease reactions, including the exonuclease activity of DNA polymerase I (*2*), staph nuclease (*3*), ribozymes (*4*), and restriction enzymes (*5*).

Type II restriction enzymes recognize, bind, and cleave four to eight base pair palindromic sequences of DNA in a metal ion-dependent manner. Since they are relatively small systems, they are natural systems for exploring the roles of

alkaline earth metals in metalloenzyme function. Mg(II) is required for phosphodiester cleavage, although Mn(II) and Co(II) can also support nuclease activity (*6, 7*). In a number of systems, Ca(II) promotes DNA binding and effective sequence discrimination (*7−10*).

We have been studying the roles of metal ions in restriction enzyme structure and function with *Pvu*II endonuclease, a homodimeric blunt-end cutter that cleaves at the central step of 5′-CAG|CTG-3′. Using isothermal titration calorimetry and ^{25}Mg NMR spectroscopy, we have established that two metal ion equivalents (Mg(II), Mn(II), or Ca(II)) bind each active site with K_d's of ∼1 mM (*11, 12*). Moreover, Ca(II) is required for avid DNA binding (*10*) and sequence discrimination (*7*). While these studies have been informative, there are some disadvantages. First, such weak metal ion binding necessitates the observation of binding behavior in the presence of high concentrations of both metal ion and enzyme. Metal ions must be present in large excess, and enzyme concentrations are often at the solubility limit. Further, many techniques involve indirect detection of bound metal ions, which means the behavior of such must be inferred.

To better understand the environments and behavior with bound metal ions, it would be advantageous to observe them directly at submillimolar spectroscopic concentrations. Lanthanide spectroscopy elegantly addresses these issues. Ln(III) ions, particularly Tb(III) and Eu(III), share many similarities with Ca(II). These ions have similar ionic radii, coordination geometries (six to eight ligands), and water exchange rates, and a strong preference for oxygen ligands (*13−15*). These similarities have led to extensive use of lanthanide luminescence spectroscopy in the study of Ca(II) binding proteins (*16−19*). Since Ca(II) and Mg(II) also share some similarities, lanthanide spectroscopy has also been applied to a few Mg(II)-dependent systems (*19−21*). Lanthanides tend to bind Ca(II)-binding proteins with affinities that are often 10^4 greater than that observed with Ca(II) (*22*), permitting the saturation of enzyme at nanomolar to micromolar concentrations. Finally, the spectral properties of the lanthanides Tb(III) and Eu(III) permit direct observation of protein-bound cations (*23*).

Recently, we demonstrated that the lanthanide ions Tb(III) and Eu(III) can promote cognate *PvuII* DNA binding as effectively as Ca(II) without supporting cleavage (*7*). This result provides us with a valuable opportunity to apply lanthanide luminescence spectroscopy in our structure−function studies of restriction enzymes. How will lanthanide ions fill *PvuII* metal ion binding sites? Can these ions be localized? Can bound metal ions be distinguished functionally and spectroscopically? A variety of lanthanide spectroscopic techniques are applied to these questions.

MATERIALS AND METHODS

Materials. Puratronic CaCl₂ was purchased from Alfa Aesar (Ward Hill, MA). EuCl₃ and TbCl₃ were purchased from Sigma Aldrich at 99.9% purity. Buffers and salts were of the highest purity and prepared with distilled deionized water. Chelex resin was purchased from Bio-Rad (Hercules, CA) and was prepared using the manufacturer's instructions. All buffers were applied to a Chelex column to remove adventitious metal ions. Subsequent pH adjustments were made with metal-free nitric acid. All solutions were determined by atomic absorption spectroscopy to be metal-free to the limits of detection (*24*).

Quantitation of Metal Ion Stocks. The concentration of Ca(II) was determined by flame atomic absorption spectroscopy using a GBC model 904BT double beam atomic absorption spectrophotometer. The quantitation of the lanthanides was conducted using standard EDTA and Arsenazo dye as previously described (*7*).

Preparation of PvuII Endonucleases. The recombinant *Escherichia coli* expression systems for wild-type and E68A *PvuII* endonuclease were kindly provided by Dr. Paul Riggs of New England Biolabs. Purification of enzyme was accomplished using phosphocellulose chromatography and heparin sepharose affinity chromatography as previously described (*25*). Proteins were concentrated using Amicon Centriprep and Centricon concentrators, and adventitious metal ions were removed via exhaustive dialysis against metal-free buffer (*26*). In repeated determinations, we have been unable to detect metal ions in enzyme samples prepared in this fashion. Thus the enzyme is referred to as "metal-free" to the limits of detection. All apoenzymes were

quantitated using $\epsilon_{280} = 36\,900$ M^{-1} cm^{-1} for the monomer subunit and handled with metal-free sterile pipet tips and sterile plasticware to prevent contamination. Routine assays of activity were performed using ³²P labeling and denaturing gel electrophoresis as previously described (*7*).

Preparation of Oligonucleotides. Unlabeled and HEX[1]-labeled oligonucleotides 5′-CAGG<u>CAGCTG</u>CGGA-3′ (featuring the cognate or specific recognition sequence) and its complement were purchased desalted from IDT Technologies (Coralville, Iowa) and purified by PAGE and Elutrap (Schleicher and Schuell, Keene, NH). With the use of Centricons, DNAs were rendered metal-free through at least two exchanges of >90% volume with deionized distilled water. Subsequent handling was accomplished with metal-free pipet tips and sterile plasticware. DNA was quantitated using ϵ_{260} values provided by the vendor. All oligonucleotide concentrations are expressed with respect to the duplex. Duplexes were formed by heating to 95 °C a mixture of 1 equiv of one strand with 1 equiv of complementary strand and permitting the sample to cool to room-temperature overnight. Samples were stored in sterile water at 4 °C for immediate use or lyophilized for storage.

Tyrosine-Sensitized Ln(III) Luminescence Spectroscopy. Tb(III) and Eu(III) luminescence emission spectra were collected on a Spex Fluorolog-3 spectrofluorimeter in either the fluorescence or phosphorescence mode. The temperature was maintained with a thermostated compartment at 25 °C. All samples were monitored with stirring using a nitric acid-cleaned quartz cuvette. The sample was excited at 274 nm, and intensity was recorded in the $^5D_4 \rightarrow {}^7F_5$ spectral range (543 nm) for Tb(III); for Eu(III), the sample was excited in the $^5D_0 \rightarrow {}^7F_2$ spectral range (282 nm), and the intensity was recorded at 614 nm. Emitted light was passed through a 450 nm cutoff filter (Andover Corp., Salem, NH) to eliminate interference from Rayleigh scattering. Tb(III) emission was monitored using both the fluorescence and phosphorescence mode. In the fluorescence mode, the band-passes were set to 5 nm. In the phosphorescence mode, the band-passes were set to 10 nm with collection parameters as follows: 100 flashes, sample window of 0.5 ms, delay after flash of 0.1 ms, and time per flash of 40 ms. When observing Eu(III) in the phosphorescence mode, the excitation band-pass was set to 14 nm, and the emission band-pass was set to 17 nm with 300 lamp flashes. To observe Ln(III) emission enhancement in the presence of the enzyme, samples containing *PvuII* monomers were titrated with a stock of LnCl₃ of known concentration. Preliminary experiments were conducted in 50 mM *N*-2-hydroxyethylpiperazine-*N*′-2-ethanesulfonic acid (HEPES), 200 mM NaCl, pH 7.5. To minimize buffer interference and maximize enzyme solubility, subsequent quantitative titration experiments were carried out in 5 mM HEPES, 400 mM NaCl, pH 7.5.

Eu(III) $^7F_0 \rightarrow {}^5D_0$ Excitation Spectroscopy. Direct excitation of Eu(III) was accomplished using a Coherent-599 tunable dye laser (0.3 nm resolution) with a Coherent Innova-70 argon ion laser as a pump source. The laser dye used in these measurements was composed of rhodamine 6G dissolved in ethylene glycol (*27*). The emission wavelength was set to 614 nm and Eu(III) excitation was monitored from

---

[1] HEX, hexachloro-fluorescein.

577 to 581.5 nm with a slit width of 8 mm. Spectra were fit using PeakFit 4.11 (Jandel Scientific, Point Richmond, CA), and the normalized intensity at 579.1 nm was plotted as a function of Eu(III) concentration. Corresponding Eu(III)−buffer corrections were conducted.

Calorimetric Analysis. Isothermal titration calorimetry was conducted on a VP-ITC Microcalorimeter (MicroCal, Northampton, MD). Measurements were controlled by MicroCal Observer software. The reference solution was distilled water purified using a MilliQ apparatus. Samples contained 10 μM monomers wild-type *Pvu*II endonuclease, 5 mM HEPES, and 400 mM NaCl, pH 7.5. The cell temperature was maintained at 25 °C by an internal Pelletier mechanism. All solutions were microfiltered and degassed prior to data collection and were stirred at 310 rpm during the experiment. Each of 40 injections of 7.5 μL of 200 μM TbCl$_3$ in 5 mM HEPES, 400 mM NaCl was delivered over 12.56 s with a 4 min equilibration time between injections. As appropriate, data from control experiments in which metal ion was injected into buffer were subtracted from all enzyme data to correct for heats of dilution. Data were processed and fit to one- and two-site binding models using MicroCal Origin software, the user's manual of which describes data analysis in detail (*28*). Isotherms were then fit to the appropriate binding model.

Metal Ion Binding Models. In the fitting of Ln(III) titration data, both one-site (eq 1) and sequential two-site (eq 2) metal ion binding models were considered:

$$EM \underset{}{\overset{K_{e_1}}{\rightleftharpoons}} M + E \qquad (1)$$

where $[EM] = [M]_f[E]_f/K_{e_1}$, $[M]_f$ is the free metal concentration, $[E]_f$ is the free enzyme concentration, and K_{e_1} is an equilibrium dissociation constant and

$$EM_2 \underset{}{\overset{K_{e_2}}{\rightleftharpoons}} EM + M \qquad (2)$$
$$\updownarrow K_{e_1}$$
$$E + M$$
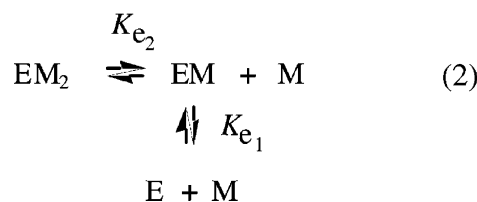
where in addition to the expression for [EM], $[EM_2] = [EM][M]_f/K_{e_2}$, where K_{e_2} is also an equilibrium dissociation constant. Finally, the lanthanide−buffer interaction was described using the expression

$$BM \underset{}{\overset{K_b}{\rightleftharpoons}} B + M \qquad (3)$$

and $[BM] = [M]_f[B_f]/K_b$, where K_b is an equilibrium dissociation constant. The program Scientist 2.01 (Micro-Math, Salt Lake City, UT) was used to simultaneously fit titration data to these equations. Total enzyme and buffer concentrations were provided to the program and fixed. The expression for total intensity features contributions from the buffer (I_b) and the enzyme (I_e), the latter of which is taken as the sum of contributions from both the primary and secondary Ln(III) binding sites. K_d's reported are averages of at least three measurements. This program was also used to calculate species distributions with given K_d's and species concentrations.
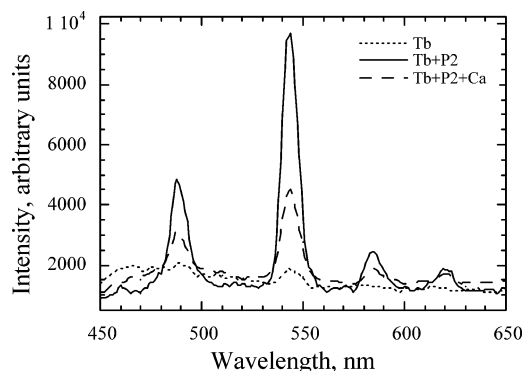

FIGURE 1: Tyrosine-sensitized Tb(III) luminescence emission spectra of 45 μM free Tb(III) (···), Tb(III) in the presence of 1 μM enzyme monomers (−, Tb + P2), and Tb(III) in the presence of enzyme and 100 mM Ca(II) (− − −, Tb + P2 + Ca). The excitation wavelength was 274 nm, the slits were set to 5 nm, and a 450 nm cutoff filter was applied to the emission monochromator. Conditions were 1 μM *Pvu*II endonuclease monomers in 50 mM HEPES, 200 mM NaCl, pH 7.5, 25 °C.

RESULTS

We have previously established that the lanthanide cations Eu(III) and Tb(III) promote DNA binding by *Pvu*II endonuclease. Like Ca(II), these ions support DNA affinities in the subnanomolar range (*7*). This behavior provides an opportunity to apply lanthanide spectroscopy to our ongoing efforts to understand restriction enzyme structure and function.

Tyrosine-Sensitized Ln(III) Luminescence Spectroscopy. The most facile of lanthanide spectroscopic experiments is tyrosine-sensitized terbium luminescence, which involves energy transfer from excited tyrosine or tryptophan to a nearby bound terbium (*29*). While quantum yields are low, this process can usually be detected using a conventional fluorimeter, is most efficient at distances up to 10 Å, and is observable in many proteins (*30*). *Pvu*II endonuclease contains four tryptophan and 10 tyrosine residues. While none of the tryptophan residues are near the active site, Tyr124 and Tyr 94 lie in the active site. The phenolic group of the former is 8 Å away from Glu68. The hydroxy group of the latter has been implicated as a Mg(II) ligand (*31*) and is 4 Å away from the critical bridging carboxylate ligand of Glu68 (*11, 12, 32*). A third tyrosine residue, 67, is adjacent to Glu68 but points away from the active site, placing the aromatic ring over 10 Å away from the carboxylate group.

Previous ¹⁹F NMR studies on fluorinated *Pvu*II endonuclease indicated that 3-fluorotyrosine residue environments were perturbed upon the addition of Ca(II) (*25*). We reasoned that one or more of these residues would be close enough to the metal ion binding site to promote energy transfer from tyrosine to enzyme-bound Tb(III). Further, even though Ca(II) binds *Pvu*II endonuclease weakly ($K_d \approx 1$ mM (*11*)), lanthanide ions tend to bind in Ca(II) sites with affinities of 10^4 M^{-1} or higher (*22*). This suggested that we could detect Tb(III) binding to *Pvu*II endonuclease at optically convenient concentrations (micro- to nanomolar). In the absence of enzyme, excitation of terbium at 274 nm yields luminescence that is barely detectable at 45 μM Tb(III) (Figure 1). However, upon the addition of 1 μM enzyme, we observe a severalfold enhancement in terbium luminescence intensity. Indeed, characteristic terbium emission lines are readily

visible at 488, 543, 584, and 619 nm. This behavior is consistent with a low micromolar affinity of the enzyme for Tb(III). An excitation maximum of 274 nm is consistent with energy transfer from tyrosine (as opposed to tryptophan, which has a higher excitation maximum (ref *29* and data not shown). Protein fluorescence emission ($\lambda_{\max} = 330$ nm) decreases as a function of added Tb(III), behavior that is consistent with energy transfer (refs *33* and *34* and data not shown). Identical experiments performed with Eu(III) produced emission spectra with peaks at 591, 615, and 692 nm and emission enhancements at 615 nm of about 3-fold (data not shown).

We have previously established that Ca(II) binds only in the enzyme active site (*11*). To confirm active site binding for Tb(III), Ca(II) was titrated into a sample of *Pvu*II endonuclease and Tb(III). Since Ca(II) binds the enzyme with K_d of 1 mM (*11*), a very large excess of this ion was necessary to compete with Tb(III). As expected, the addition of Ca(II) reduced the enhancement of terbium luminescence; this behavior is most easily observed at 488 and 543 nm (Figure 1). This result is consistent with Tb(III) binding in approximately the same manner as Ca(II), that is, in the active site.

Eu(III) Excitation Spectroscopy. Europium excitation spectroscopy is well established as an informative technique for observing metal ion environments in macromolecules (*23*). Upon direct excitation, Eu(III) undergoes a $^7F_0 \rightarrow {}^5D_0$ transition, which is most typically observed as excitation spectra. The use of tunable laser excitation permits direct observation of this transition, as well as the ability to discriminate among different binding sites. The latter characteristic is due to the intrinsic sharpness of this transition and the fact that the energy of the transition may vary with chemical environment.

We began by titrating Eu(III) into parallel samples of buffer and 20 μM enzyme monomers, observing changes in the excitation spectra as a function of added Eu(III). As highlighted in Figure 2A, the dominant feature of this spectrum is a peak centered at 579.2 nm. Since this peak is only observed when enzyme is present, it is assigned to that of enzyme-bound Eu(III). As the concentration of Eu(III) is increased to 40 μM, another peak centered at 578.7 nm becomes obvious. To assign this peak, a series of control spectra were collected at 150 μM Eu(III). As shown in Figure 2B, only the peak at 578.7 nm is observed in the absence of enzyme; however, since it is not present in water, it is assigned to HEPES-bound Eu(III). We believe the peak representing Eu(III)—buffer interactions is easily visible in these experiments because relative to other lanthanide-substituted protein systems, our enzyme concentrations are high and *Pvu*II endonuclease-bound Eu(III) signals are weak (G. Muller, unpublished observations). While we do not know the exact reason for this, we speculate that the protein environment could contribute to some quenching behavior.

To confirm the location of Eu(III) in the active site, two experiments were performed. First, an excess of Ca(II) was titrated into a sample of enzyme and Eu(III). As shown in Figure 3, decreasing intensity at 579.2 nm was observed. This response indicates that Ca(II) and Eu(III) bind competitively, confirming active site binding for Eu(III). Multiple titrations were conducted using both Eu(III) excitation and tyrosine-sensitized phosphorescence spectroscopies. The data
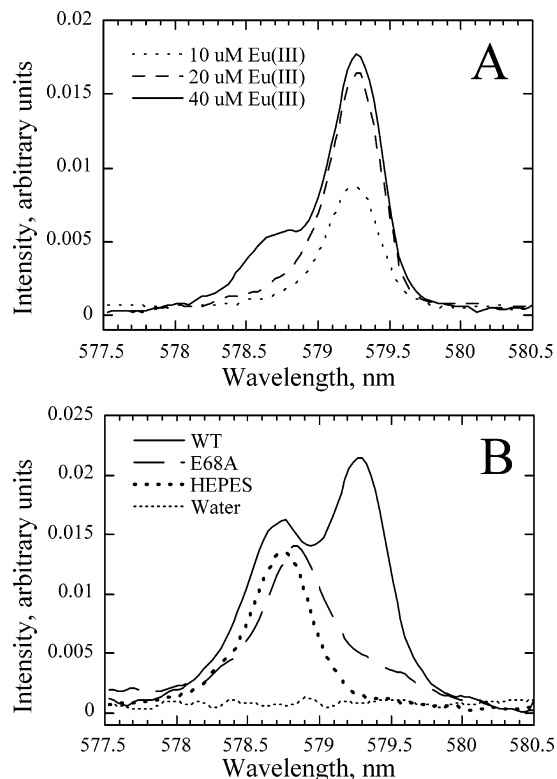

FIGURE 2: $^7F_0 \rightarrow {}^5D_0$ excitation spectroscopy of Eu(III): (A) 20 μM *Pvu*II monomers in the presence of increasing Eu(III) as indicated in the inset; (B) 150 μM Eu(III) in water, in 5 mM HEPES, and in the presence of 20 μM wild-type and E68A *Pvu*II endonuclease monomers. Symbols are as indicated in the inset. Unless otherwise specified, the conditions are 5 mM HEPES, 400 mM NaCl, pH 7.5, 25 °C. The excitation wavelength is 615 nm, and the slits are at 8 mm. These data are both power- and dilution-corrected.
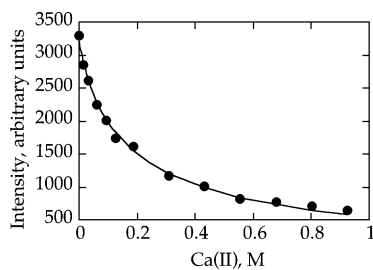

FIGURE 3: Ca(II) displacement of enzyme-bound Eu(III) as observed by tyrosine-sensitized Eu(III) phosphorescence spectroscopy. Conditions were 10 μM enzyme monomers, 20 μM Eu(III), 5 mM HEPES, 400 mM NaCl, pH 7.5, 25 °C. Europium emission intensity was observed at 614 nm. The data were fit to an equilibrium competition model to yield an apparent $K_{d,app}$ for Eu(III) of 0.7 $\pm$ 0.3 μM and a $K_{d,app}$ for Ca(II) of 2.6 $\pm$ 0.6 mM.

fit easily to an equilibrium competition model to yield an apparent K_d of 0.7 $\pm$ 0.3 μM for Eu(III) and a K_d of 2 $\pm$ 0.6 mM for Ca(II), the latter of which agrees with that previously published (*11*). In a second experiment, Eu(III) excitation spectra were collected in the presence of the active site variant E68A. This variant displays only residual DNA cleavage activity. Multiple thermodynamic experiments indicate that binding of 2 equiv of Ca(II), Mn(II), or Mg(II) is severely compromised in this variant, thus implicating Glu68 as a bridging ligand (*11, 12*). As shown in Figure 2B, the intensity at 579.2 nm is greatly diminished, appearing only as a broad shoulder of a larger peak centered at 578.8 nm. The proximity of this peak to that attributed to the
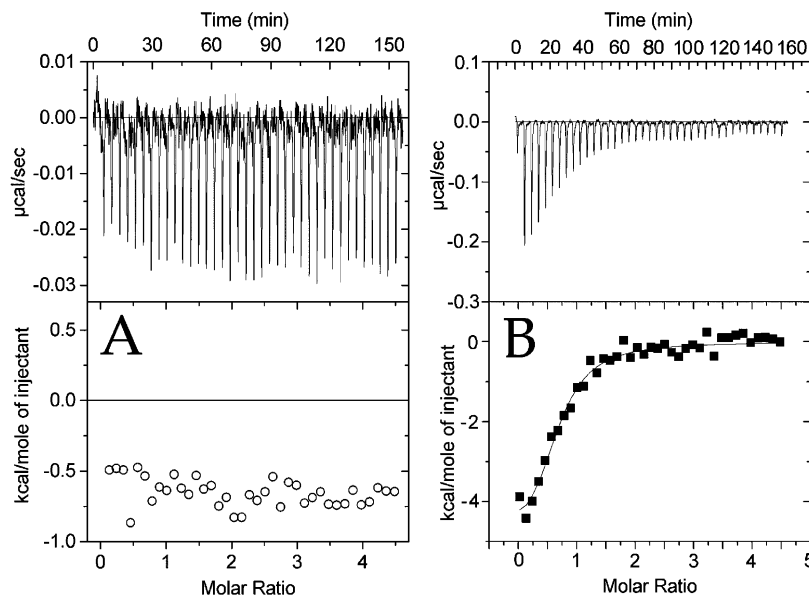
FIGURE 4: Isothermal calorimetric binding studies of Tb(III) binding by *Pvu*II endonuclease: (A) titration of buffer with 40 × 7.5 *μ*L injections of Tb(III) (note the very shallow scale of the titration); (B) titration of 10 *μ*M enzyme monomers with 40 × 7.5 *μ*L injections of Tb(III). Experiments were performed in 5 mM HEPES, 400 mM KCl at 25 °C, pH 7.5, with a Tb(III) stock of 200 *μ*M. Application of both one- and two-site models were consistent with the titration of one site with a $K_{d,app}$ of 2 *μ*M.

Eu(III)−buffer interaction suggests two possibilities: (i) The mutation has caused Eu(III) to partition to the buffer, consistent with a very deleterious effect of the mutation on Eu(III) binding. A more detailed examination of this possibility appears below. (ii) Eu(III) binds E68A in a nonspecific manner in an environment that is similar to the buffer. This peak appears to differ slightly in position from the buffer peak ($\Delta\lambda_{max} \approx 0.1$ nm); since the direction of the shift (blue vs red) varies from sample to sample and the magnitude is at the detection limit, it is not interpreted. Altogether, the data confirm the importance of Glu68 to Eu(III) binding.

Quantitative Analysis of Lanthanide Binding. In our quest to understand metal ion environments and possibly to use lanthanide spectroscopy to probe endonuclease mechanism, we are of course interested in establishing metal ion affinities and stoichiometries. Previous studies of *Pvu*II endonuclease indicated that Ca(II), Mn(II), and Mg(II) all bind the enzyme with a stoichiometry of two metal ions per monomer (*11, 12*). Size alone should not prohibit the binding of 2 equiv of Ln(III) ion per active site. Hexacoordinate Ca(II) has an ionic radius of 1.14 Å (*35*). Lanthanide ions usually exhibit *n* + 1 coordination number relative to Ca(II); heptacoordinate Tb(III) and Eu(III) have ionic radii of 1.12 and 1.15 Å, respectively (*35*). However, as lanthanide substitution in other metalloenzyme systems indicates (*19, 36*), other factors can clearly be significant (see Discussion).

An important consideration is the detection of lanthanide−buffer interactions, which are obvious in both tyrosine-sensitized luminescence and Eu(III) excitation luminescence spectroscopies. Metal ion interactions with buffers commonly used in lanthanide spectroscopy (e.g., HEPES, 3-(*N*-morpholino)propanesulfonic acid (MOPS), piperazine-1,4-bis (2-ethanesulfonic acid) (Pipes), Tris) are typically weak. For many systems, this is not a concern; however, as mentioned above, signal intensities arising from lanthanide−*Pvu*II endonuclease are smaller than for some proteins. For this reason, we chose to collect Eu(III) excitation spectra at 10−20 *μ*M enzyme monomers, a concentration that is relatively

high compared to those used for other systems. Further, to preserve pH during titrations, the buffer is in a large molar excess, a condition that can favor weak interactions in dilute protein solutions.

The issue of lanthanide−buffer interactions was addressed in a number of ways. First, binding affinities of both the enzyme and buffer for Tb(III) were investigated by isothermal titration calorimetry. While measurements with Eu(III) would clearly be most relevant to excitation measurements, the enzyme is more soluble at higher concentrations of Tb(III). As shown in Figure 4A, the heat released upon the addition of Tb(III) to HEPES is negligible; thus, the titration data in Figure 4B reflect the Tb(III)−enzyme interaction. Application of both one- and two-site binding models were consistent with one binding site with a $K_{d,app}$ of 2 *μ*M. In addition, monitoring of titrations of Eu(III) into *Pvu*II endonuclease via phosphorescence spectroscopy, with which there is no detectable buffer signal, produced a $K_{d,app}$ of 4 *μ*M. These binding constants are very similar to those obtained for other lanthanide-substituted systems (*16, 19, 37*).

While one can clearly make measurements that do not produce signals resulting from the lanthanide−buffer interaction, the equilibrium can still affect lanthanide−enzyme interactions. To address this issue, titration data were collected for both ions using tyrosine-sensitized lanthanide spectroscopy. At 10−20 *μ*M enzyme monomers, data points could often be obtained to   100 *μ*M Ln(III) before the enzyme precipitated. Luminescence enhancements for both Tb(III) and Eu(III) yielded titration curves such as those shown in Figure 5. In addition to a simple one-site model, these uncorrected data were then applied to a two-site competition model (*38*), which describes both metal ion−buffer and metal ion−enzyme equilibria (see Materials and Methods). Apparent dissociation constants for the enzyme−metal interaction (2 or 4 *μ*M, as appropriate) and the buffer−metal interaction (5 mM, estimated via luminescence spectroscopy) were used to guide the fitting. The results of these fits are summarized in Table 1. For both ions, the data fit
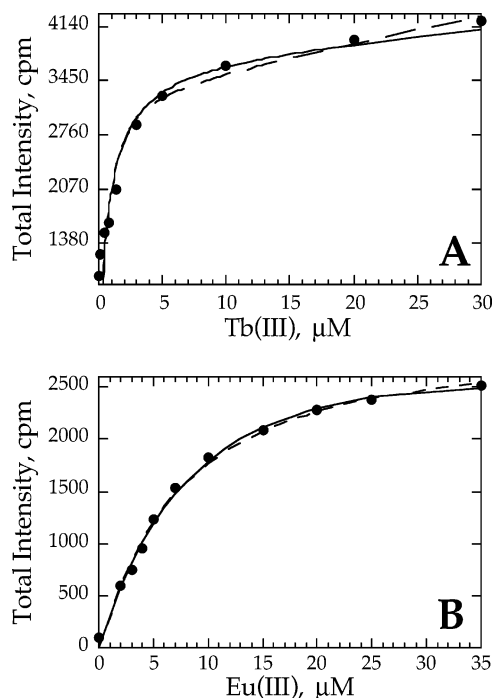
FIGURE 5: Lanthanide binding isotherms as measured by tyrosine-sensitized luminescence spectroscopy: (A) titration of Tb(III) into 750 nM enzyme monomers (to facilitate evaluation of behavior early in the titration, points at higher metal ion concentrations are not shown); (B) titration of Eu(III) into 2.5 μM enzyme monomers. One- (− − −) and two-site (—) binding models were applied to several data sets to yield the values in Table 1. Conditions were 5 mM HEPES, 400 mM NaCl, pH 7.5, 25 °C; for Tb(III), λ_{ex} = 274 nm, and λ_{em} = 543 nm; for Eu(III), λ_{ex} = 282 nm, and λ_{em} = 614 nm.

Table 1: Summary of Mathematical Fitting of *Pvu*II Ln(III) Binding Behavior[a]

model	parameter	Tb(III)/WT	Eu(III)/WT	Eu(III)/E68A
single	$K_{d,app}$, M	$(1.1 \pm 0.6) \times 10^{-6}$	$(3.3 \pm 2.3) \times 10^{-6}$	100×10^{-6} [b]
	R^2	0.986	0.997	
sequential	K_{e_1}, M	$(2.3 \pm 1.7) \times 10^{-6}$	$(1.4 \pm 0.6) \times 10^{-6}$	
two-site	K_{e_2}, M	$(117 \pm 46) \times 10^{-6}$	$(223 \pm 161) \times 10^{-6}$	
	K_b, M	$(4.7 \pm 1.6) \times 10^{-3}$	$(3.9 \pm 2.9) \times 10^{-3}$	
	R^2	0.988	0.998	

[a] Titration data were obtained using tyrosine-sensitized luminescence spectroscopy and fit to apparent single-site and sequential two-site multiple equilibria models as described in Materials and Methods. K_{e_1} and K_{e_2} are enzyme−metal dissociation constants, and K_b is the lanthanide−buffer dissociation constant. K_d's are an average of at least three measurements. Conditions were 5 mM HEPES, 400 mM NaCl, pH 7.5, 25 °C. [b] Estimated from the isotherm, which did not reach saturation.

comparably well to both single-site and two-site sequential models with K_d's for a primary site in the low micromolar range. For both ions, a second weaker site titrates with K_d's of 100−200 μM. Calculation of species distribution under experimental conditions (Figure 6 and Table 2) indicates that the second site is less than 17% occupied below 35 μM Ln(III); this explains why fits to these models are comparable at low metal ion concentrations.

Now that useful multiple equilibria models have been developed, they can also be used to verify a partitioning of Eu(III) to the buffer in the presence of E68A. Isotherms in the presence of this variant are quite shallow. While this weakened binding and solubility limits hamper the collection
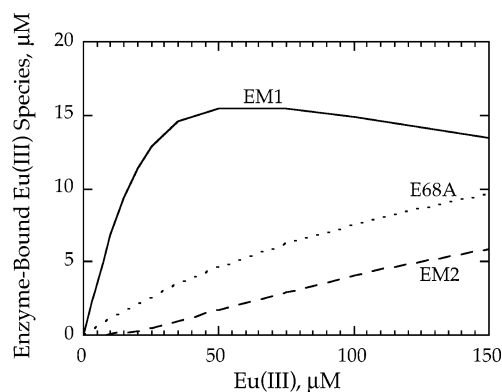

FIGURE 6: Distribution of enzyme-bound Eu(III) species as a function of Eu(III) concentration: wild-type strong site (EM1, —); wild-type weak site (EM2, − − −); E68A (•••). Data were simulated using the K_d values in Table 1.

Table 2: Summary of Peak Fitting and Population Distribution Calculations[a]

spectrum	wavelength, nm	relative area, % — 150 μM Eu(III)	fractional occupancy[b] — 150 μM Eu(III)	fractional occupancy[b] — 35 μM[d] Eu(III)
wild-type	578.70			
	579.23	72.4 [c]	0.674	0.729
	579.39	27.6 [c]	0.295	0.047
E68A	578.83			
	579.47		0.484	0.174
HEPES	578.73			

[a] The data presented here was obtained from the spectral data in Figure 7. Conditions: 20 μM enzyme monomers, 5 mM HEPES, 400 mM NaCl, pH 7.5, 25 °C at the Eu(III) concentrations indicated. [b] Fraction of each site occupied under experimental conditions, as demonstrated using the equilibrium constants summarized in Table 1 and the sequential two-site binding model described in Materials and Methods. Peak assignments are based upon the correlation between the relative areas of excitation peaks and fractional occupancies of thermodynamically determined metal ion binding sites. [c] Calculated based on peaks attributed to enzyme binding at 150 μM Eu(III). [d] Concentration at which the strong site is well populated but the weak site is not.

of a high-quality isotherm, $K_{d,app}$ for Eu(III)−E68A is estimated to be $\geq$100 μM. The distribution of species were simulated using this value and the 5 mM K_d value for the Eu(III)−buffer interaction. At 20 μM E68A monomers and 150 μM Eu(III), less than half of the enzyme is bound by Eu(III) (Figure 6). While we cannot rule out additional nonspecific interactions with the enzyme, the peak at 578.7 nm is most likely due to the Eu(III)−buffer interaction.

Line Shape Analysis. To determine whether multiple enzyme-bound Eu(III) environments could be distinguished, we performed a line shape analysis of the Eu(III) excitation spectra. At 150 μM Eu(III), the dominant Eu−enzyme peak fits well to two peaks with an area ratio of 72/28 (Figure 7A, Table 2). A comparable occupancy ratio is obtained when determining the distribution of species at 150 μM Eu(III) using the experimentally determined K_d's and the multiple equilibrium model described above. At 35 μM Eu(III), a concentration at which the strong site is well populated but the weak site is not, the relative intensity of the smaller peak corresponds with the modest level of occupancy expected with the determined K_d's. These data are therefore consistent with the above two-site model.
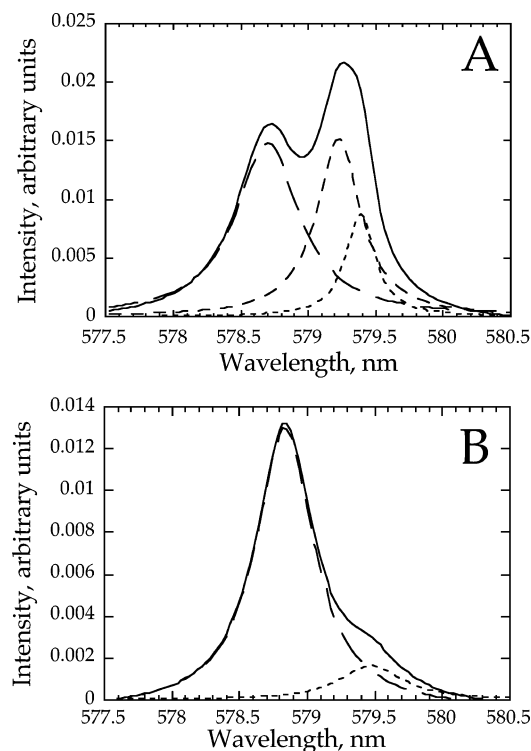
FIGURE 7: Line shape analysis at 150 μM Eu(III) for (A) wild-type *Pvu*II endonuclease (experimental data (—) fit to three peaks (− − −) at 578.70, 579.23, and 579.39 nm and (B) E68A *Pvu*II endonuclease (experimental data (—) fit to two peaks (− − −) at 578.83 and 579.47 nm. A spectrum collected in buffer alone featured a peak at 578.73 nm. See Table 2 for additional details. Conditions were 20 μM enzyme monomers, 5 mM HEPES, 400 mM NaCl, pH 7.5, 25 °C.

Additional evidence for the second site is evident in Eu(III) excitation spectra of E68A. At high Eu(III) concentrations, a peak is evident at 579.5 nm, a location very comparable to the smaller, higher wavelength peak in the wild-type spectrum. Thus Glu68 is not important for Eu(III) binding at this secondary site.

Functional Importance of Weak Ln(III) Binding Site. While the above data are consistent with two Ln(III) binding sites, the low occupancy of the second site makes it difficult to detect in these experiments. This prompted us to confirm this site by other means. The simplest way to do this is to perform a titration at high micromolar enzyme and Ln(III) concentrations. However, despite multiple attempts, the enzyme precipitates under these conditions.

Since this weaker site cannot be directly observed with this approach, we sought to infer the existence of this site indirectly. Previously we noted the sigmoidal dependence of DNA binding on Ca(II) concentration and used this information to demonstrate that two Ca(II) ions participate in DNA binding (*39*). We reasoned that the Ln(III) dependence of substrate binding could be used to determine whether multiple lanthanide equivalents are important to this process. This would in turn provide evidence for a second Ln(III) binding site. DNA binding constants at various Eu(III) and Tb(III) concentrations are summarized in Table 3. At 1 μM Ln(III), dissociation constants for the enzyme binding its target sequence are 3 nM for Tb(III) and 44 nM for Eu(III). However, we have previously established that in the presence of 1 mM Tb(III) and above, the enzyme binds its target sequence with subnanomolar affinity (*7*). We confirm

Table 3: Metal Ion Dependence of DNA Dissociation Constants for Wild-type and E68A *Pvu*II[a]

metal	metal concn	DNA K_d, M
	Wild-type	
Ca(II)[b]	100 μM[b]	$(36 \pm 5) \times 10^{-9}$
	1 mM[b]	$(244 \pm 162) \times 10^{-12}$
	10 mM[b]	$(82 \pm 61) \times 10^{-12}$
Tb(III)	1 μM	$(3.2 \pm 1.2) \times 10^{-9}$
	10 μM	$(2.9 \pm 2.5) \times 10^{-9}$
	100 μM[b]	$(617 \pm 140) \times 10^{-12}$
	1 mM[b]	$(267 \pm 236) \times 10^{-12}$
	10 mM[b]	$(56 \pm 11) \times 10^{-12}$
Eu(III)	1 μM	$(44 \pm 9) \times 10^{-9}$
	10 μM	$(3.8 \pm 0.1) \times 10^{-9}$
	100 μM	$(100 \pm 36) \times 10^{-12}$
	1 mM	$(119 \pm 40) \times 10^{-12}$
metal-free[b]		$(0.53 \pm 0.39) \times 10^{-6}$
	E68A	
Ca(II)	1 mM[b]	$(6.2 \pm 4.6) \times 10^{-6}$
	10 mM[b]	$(118 \pm 43) \times 10^{-9}$
Eu(II)	1 mM	48×10^{-9c}
Tb(III)	1 mM[b]	$(135 \pm 58) \times 10^{-9}$
metal-free[b]		$(1.9 \pm 0.8) \times 10^{-6}$

[a] All values are averages of at least three measurements. Conditions were, unless otherwise noted, 50 mM Tris, 100 mM NaCl, 10 mM metal ion at pH 7.5, 25 °C. All measurements made at concentrations lower than 10 mM metal ion were adjusted to constant ionic strength with the addition of an appropriate amount of NaCl. [b] Taken from ref *7*. [c] Isotherm did not plateau before reaching enzyme solubility limit.

that this is also the case for Eu(III) (Table 3). Thus there is a 38-fold decrease in K_d between 10 and 100 μM Eu(III). A similar though less pronounced effect is observed for Tb(III). In both cases, increased affinity for DNA at high Ln(III) concentrations is consistent with a second, weaker Ln(III) binding site; moreover, this second site is clearly important to avid DNA binding.

Similar experiments with E68A provide additional evidence for this model. This active site variant binds alkaline earth metals very poorly (K_d for Mg(II) $\approx$ 40 mM (*12*)). However, while the removal of the Glu68 side chain severely compromises tight Ln(III) binding at low micromolar concentrations, E68A does indeed bind Ln(III) ions at submillimolar concentrations ($K_d \approx$ 100 μM; Table 1). If the weaker binding metal ion site is preserved in E68A but is still important to DNA binding, this activity should be stimulated in this variant relative to metal-free conditions. While Nastri et al. were unable to observe DNA binding by E68A in the presence of Ca(II) using the gel mobility shift assay (*40*), the determination of DNA binding constants using HEX-labeled oligonucleotides and fluorescence anisotropy affords a wider range of working concentrations. This permits the detection of DNA binding constants in the low micromolar range (*10*). As predicted by the model, Ln(III) ions do indeed stimulate DNA binding by this variant (Table 3). At 1 mM Tb(III), E68A binds DNA with a K_d of 135 nM, representing a 15-fold increase in affinity relative to metal ion independent binding (Table 3). Although solubility difficulties hamper measurements with Eu(III), E68A behavior in the presence of this lanthanide ion appears to be similar.

DISCUSSION

While the alkaline earth metal ions Mg(II) and Ca(II) are the most abundant divalent metal ions in cells (*41*), they lack many of the intrinsic spectroscopic handles of the less

abundant transition metal ions. This has necessitated the application of metal ion substitution, in which metal ions with similarities to these ions are used as probes. Among ions used to replace Ca(II), lanthanide ions are especially advantageous: First, they share with Ca(II) similar ionic radii, coordination geometries (six to eight ligands), water exchange rates and a strong preference for oxygen ligands (*7*, *13−15*). Second, lanthanides are luminescent, providing useful spectroscopic tools for understanding metal ion environments in metal complexes and macromolecules (*22*, *23*, *42*, *43*). These properties have led to extensive use of lanthanides and lanthanide spectroscopy in the study of Ca(II) binding proteins. Those studied in this fashion include calmodulin (*16*), parvalbumin (*17*), protein kinase C (*18*), and Klenow fragment of DNA polymerase I (*19*). Such studies have been useful in identifying and characterizing metal ion binding sites (*23*). While Mg(II) and Ca(II) also share some similarities in geometry and ligand preference (*41*), Mg(II) is appreciably smaller (0.9 Å ionic radius (*35*)) than either Ca(II) or lanthanide ions. This is perhaps the central reason that lanthanide substitution and lanthanide spectroscopy have been less extensively applied to Mg(II) binding systems. Nevertheless, this technique has been applied to nucleic acids; recent studies include those of hairpin loops (*44*) and the hammerhead ribozyme (*21*).

Since restriction enzymes utilize both Ca(II) and Mg(II) in their functions, performing Ln(III) substitution and lanthanide spectroscopy on these enzymes is a natural extension of these efforts. Based on both crystallographic and functional data, two metal ion mechanisms have been proposed for a number of these systems (*5*); further details regarding the hydrolytic mechanism, in particular the involvement of each metal ion in the reaction, remain elusive. For the model system *Pvu*II endonuclease, we have established that 2 equiv each of Mg(II), Ca(II), and Mn(II) bind *Pvu*II endonuclease with low millimolar affinities (*11*, *12*), K_d values that are typical for nucleases (*11*). In applying various binding models to the free enzyme, the affinities of the two sites for these ions were indistinguishable and do not appear to be strongly coupled. These properties make it difficult to probe individual sites.

We reasoned that further insights might emerge from functional studies. In an effort to determine whether both equivalents of metal ion were needed for DNA binding, we determined the metal ion dependence of DNA binding using Ca(II). Between 0 and 1 mM Ca(II), the K_a for DNA binding increases 100-fold; between 1 and 5 mM, it increases another 30-fold. The sigmoidal dependence of DNA K_a on Ca(II) is consistent with a requirement of two metal ions for DNA binding (*39*). While these experiments provided a means of distinguishing metal ions, the lack of spectroscopic handles and weak metal ion affinities make further exploration of these sites problematic.

The similarities between Ca(II) and lanthanide ions prompted us to examine the potential of the latter as cofactors for *Pvu*II endonuclease. Tb(III) and Eu(III) were found to stimulate DNA binding in a manner very similar to Ca(II) (*7*). Since these ions tend to bind proteins more tightly than Ca(II) or other alkaline earth metal ions (*22*), we reasoned that it might be possible to use these ions to observe enzyme−metal ion complexes at lower enzyme concentrations, facilitating the discrimination of sites.

As summarized above, Eu(III) excitation data fit to a two-site binding model featuring one strong (low micromolar) and one weak (high micromolar) Ln(III) binding site, Glu68 being a critical ligand for the former. Another indication of two sites came from fitting data to the Hill equation in which the order with respect to the metal is a variable (*39*). When a metal ion titration is conducted at low enzyme concentrations (<1 μM), the data fit to Hill numbers near one per enzyme monomer. When fitting metal ion titration data collected at higher enzyme concentrations (2−10 μM), Hill coefficients were consistently closer to two per enzyme monomer. The most dramatic evidence for a second, weaker site emerged in the dependence of substrate binding on Ln(III) ion concentration: DNA binding affinities in the presence of Ln(III) dramatically increase around 100 μM metal ion.

A system that features strong and weakly binding Ln(III) sites is not without precedent. Our Eu(III) spectral data are remarkably similar to those observed for the EF hand protein S100β (*37*). In this system, both strong and weak Eu(III) sites were detected about 12 Å apart; moreover, the Eu(III) excitation spectrum of this system, which features one large peak and a smaller, slightly shifted peak, is quite similar to that presented here.

Geometric Considerations. The lanthanide binding model proposed for *Pvu*II endonuclease prompts a number of important questions. First, does the second metal ion bind in the active site? While no direct evidence of this has been presented, the fact that DNA binding is stimulated 35-fold between 10 and 100 μM lanthanide, concentrations above the K_d for the tight site, is consistent with binding somewhere in the active site. In some respects, the nonlinear dependence of DNA binding on Ln(III) concentration is similar to that observed with Ca(II), albeit in a lower concentration range (*39*). While an allosteric site is possible, it seems unlikely that such an arrangement would drive DNA binding as avid as is observed here (10⁻¹¹ M). Second, is there sufficient space and ligands for an additional equivalent of lanthanide in the active site? As mentioned previously, 2 equiv of Ca(II) binds in the active site of *Pvu*II endonuclease and a number of other restriction enzymes (*5*). Heptacoordinate Eu(III) and Tb(III) are similar in size to hexacoordinate Ca(II) (vide supra (*35*)). In addition, a heavy atom derivative of *Pvu*II endonuclease features one Pr(III) ion (radius 1.2 Å (*35*)) and one large, negatively charged sulfate ion (2.3 Å radius (*45*)) in the active site (1K0Z.pdb). Finally, our earlier NMR studies indicate that *Pvu*II endonuclease has shown remarkable conformational plasticity in the binding of large metal ions (*25*). These data indicate that from the standpoint of size alone, two Ln(III) ions can be accommodated in the active site.

A more critical issue for the binding of two Ln(III) ions in the *Pvu*II active site is the distribution of ligands. In previous studies, we identified Glu68 as a bridging ligand between two Ca(II) ions (*11*). The structure of *Pvu*II endonuclease in the presence of both Ca(II) and DNA confirms this result (*32*). A more recent structure of an enzyme−Mg(II) complex at pH 5.0 (notably below the $pK_{a,app}$ for Mg(II) binding (*12*)) reveals single metal ion sites in two different arrangements. In one subunit, one Mg(II) ion is ligated by Glu68 and Asp58; in the other, one Mg(II) ion is ligated by the hydroxyl group of Tyr94 (*31*).

Since we observe here that Glu68 is not required to bind Ln(III) at the weak site, it follows that this residue does not serve as a bridging ligand for these ions. While the arrangement of one strong site is reminiscent of the latter structure mentioned above, the geometry is more likely dominated by the potential of lanthanides to bind up to nine ligands. This behavior is in contrast to that of alkaline earth metals Mg(II) and Ca(II), which typically bind six ligands. Thus it follows that for Ln(III), there are fewer ligands available for the second metal ion equivalent. This would be consistent with weakened binding relative to the stronger site, and indeed, this is what is observed: The second Ln(III) ion binds the enzyme 100-fold more weakly than the first equivalent. While there is little quantitative information regarding how DNA binding affects enzyme−metal interactions, it seems reasonable that DNA could provide additional oxygen ligands to stabilize the second site.

There are a number of multinuclear metalloenzyme systems to which lanthanide substitution and lanthanide spectroscopy have been applied. The most classic is calmodulin, perhaps the best studied Ca(II)-binding protein. Each lobe of calmodulin binds two Ca(II) ions, located about 12 Å apart. Lanthanide spectroscopists have simultaneously substituted both sites with Eu(III) (*46*). The protease thermolysin has a number of metal ion binding sites, two of which are separated by only a few angstroms. In an early crystallographic study of lanthanide substitution, one lanthanide ion filled the dinuclear site (*36*). The system most similar to *Pvu*II endonuclease to which lanthanide spectroscopy has been applied is the Klenow fragment of *E. coli* polymerase I. While two metal ion binding sites have been identified by X-ray crystallography (*2*), the functional relevance of a second metal ion binding site has been challenged (*47*). For this system, both spectroscopy and crystallography revealed the dinuclear site as being filled with one lanthanide, albeit in two configurations (*19*, *48*). Interestingly, both oxygen atoms of Asp355 ligate to a single Eu(III) ion. The configuration of the site was attributed to the high coordination number of lanthanide ions. While there are a number of small ligand complexes that feature dinuclear lanthanide complexes (*49*, *50*), the above data suggest that proximal binding of two Ln(III) ions to a protein is fairly unusual.

The fact that there are no known examples of dinuclear Ln(III) sites in proteins prompted us to consider an alternate interpretation for our data. When two excitation peaks have been detected but binding isotherms are consistent with one Ln(III) binding equivalent, a mixture of configurational isomers has been proposed (*19*). For this model to apply here, there would have to be impetus for a shift in the position of Ln(III) at higher metal concentrations from the tighter site to the weaker site. This scenario would require some additional thermodynamic driving forces, which might come in the form of DNA binding, enzyme conformational changes, or both. Finally, this second site would not rely on Glu68 as a critical ligand, even though in this scenario the tighter site requiring this ligand would no longer exist or be occupied. Finally, it is not consistent with the higher Hill coefficients mentioned above.

The complexity and thermodynamic requirements of this alternate interpretation make the simpler explanation of one strong and one weak site more attractive. How is this rationalized in light of the existing literature? Much of the published lanthanide spectroscopic data is collected at low micromolar concentrations. This is probably because for most systems, the optical signal-to-noise ratio is reasonable in this range and tight Ln(III) binding constants are easily obtained. A consequence of working at these concentrations is that observations are limited to sites with K_d's in the same range. It is entirely plausible that for a number of systems, secondary sites that are not significantly occupied at common experimental concentrations may indeed exist. The relatively weak signal-to-noise ratio for *Pvu*II-bound Eu(III) encouraged us to work at higher enzyme concentrations (10−20 μM). In addition to making the Ln(III)−buffer signal more obvious, these conditions permitted the population of weaker sites. While enzyme solubility limits preclude spectroscopy under conditions that would *saturate* a weak site, we are fortunate to have a system in which Ln(III) ions promote function (i.e., DNA binding). Since DNA binding is avid at high Ln(III) concentrations, enzyme concentrations in these assays (<10 nM enzyme dimers) are well below the solubility limit. Without these functional studies conducted at higher lanthanide concentrations, evidence for the weak site would be less convincing.

CONCLUSION

Elucidating metal ion environments and how respective metal ions contribute to function are particular challenges in studying alkaline earth-dependent metalloenzymes. The two-metal-ion active site and its suitability for Eu(III) excitation spectroscopy has rendered *Pvu*II endonuclease an informative Ln(III) system. These properties have permitted the examination of competitive Ln(III)−buffer effects and, more importantly, led to the simultaneous detection of a low micromolar affinity Ln(III) site and a secondary, weaker Ln(III) binding site, both of which are important to avid DNA binding. These results suggest that weak secondary Ln(III) sites in other metalloenzyme systems might also be accessible through this unique combination of spectroscopic and functional assays. In addition, the large difference in binding affinities for these two sites should make it possible to identify and preferentially fill particular sites and observe them individually. The increased affinity over alkaline earth metal ions also provides opportunities for a variety of mixed metal ion experiments. These strategies should prove useful in ongoing endonuclease structure−function studies.

REFERENCES

1. Cowan, J. A. (1997) *Inorganic Biochemistry, an Introduction*, Wiley-VCH, New York.
2. Beese, L. S., and Steitz, T. A. (1991) Structural basis for the 3′-5′ exonuclease activity of *Escherichia coli* polymerase I: A two metal ion mechanism, *EMBO J. 10*, 25−33.
3. Suck, D., Oefner, C., and Kabsch, W. (1984) Three-dimensional structure of bovine pancreatic DNase I at 2.5 Å resolution, *EMBO J. 3*, 2423−2430.
4. DeRose, V. (2003) Metal ion binding to catalytic RNA molecules, *Curr. Opin. Struct. Biol. 13*, 317−324.

5. Pingoud, A., and Jeltsch, A. (2001) Structure and function of type II restriction endonucleases, *Nucleic Acids Res. 29*, 3705−3727.

6. Gormley, N. A., Bath, A. J., and Halford, S. E. (2000) Reactions of *Bgl*I and other type II restriction endonucleases with discontinuous recognition sites, *J. Biol. Chem. 275*, 6928−6936.

7. Bowen, L. M., and Dupureur, C. M. (2003) Investigation of restriction enzyme cofactor requirements: A relationship between metal ion properties and sequence specificity, *Biochemistry 42*, 12643−12653.

8. Vipond, I. B., and Halford, S. E. (1995) Specific DNA recognition by *Eco*RV restriction endonuclease induced by calcium ions, *Biochemistry 34*, 1113−1119.

9. Lagunavicius, A., Grazulis, S., Balciunaite, E., Vainius, D., and Siksnys, V. (1997) DNA binding specificity of *Mun*I restriction endonuclease is controlled by pH and calcium ions: Involvement of active site carboxylate residues, *Biochemistry 36*, 11093−11099.

10. Conlan, L. H., and Dupureur, C. M. (2002) Dissecting the metal ion dependence of DNA binding by *Pvu*II endonuclease, *Biochemistry 41*, 1335−1342.

11. José, T. J., Conlan, L. H., and Dupureur, C. M. (1999) Quantitative evaluation of metal ion binding to *Pvu*II restriction endonuclease, *J. Biol. Inorg. Chem. 4*, 814−823.

12. Dupureur, C. M., and Conlan, L. H. (2000) A catalytically deficient active site variant of *Pvu*II endonuclease binds Mg(II) ions, *Biochemistry 39*, 10921−10927.

13. Martin, R. B. (1984) in *Metal Ions in Biological Systems* (Sigel, H., Ed.) Vol. 17, pp 32−49, Marcel Dekker, New York.

14. Moeller, T. (1963) *The Chemistry of the Lanthanides*, Reinhold, New York.

15. Martell, A. E., and Smith, R. M. (1989) *Critical Stability Constants*, Plenum, New York.

16. Bruno, J., Horrocks, W. D., Jr., and Zauhar, R. J. (1992) Europium(III) luminescence and tyrosine to terbium(III) energy-transfer studies of invertebrate (octopus) calmodulin, *Biochemistry 31*, 7016−7026.

17. Henzl, M., Trevino, C., Dvorakov, L., and Boschi, J. (1992) Evidence that deprotonation of serine-55 is responsible for the pH-dependence of the parvalbumin Eu^{3+} $^7F_0 \rightarrow {}^5D_0$ spectrum, *FEBS Lett. 314*, 130−134.

18. Walters, J. D., and Johnson, J. D. (1990) Terbium as a luminescent probe of metal-binding sites in protein kinase C, *J. Biol. Chem. 265*, 4223−4226.

19. Frey, M. W., Frey, S. T., Horrocks, W. D., Jr., Kaboord, B. F., and Benkovic, S. J. (1996) Elucidation of the metal-binding properties of the Klenow fragment of *Escherichia coli* polymerase I and bacteriophage T4 DNA polymerase by lanthanide(III) luminescence spectroscopy, *Chem. Biol. 3*, 393−403.

20. Lin, W., Dombrosky, P., Atkins, W., and Villafranca, J. (1991) Terbium(III) luminescence study of tyrosine emission from *Escherichia coli* glutamine synthetase, *Biochemistry 30*, 3427−3431.

21. Feig, A., Panek, M., Horrocks, W. D., Jr., and Uhlenbeck, O. (1999) Probing the binding of Tb(III) and Eu(III) to the hammerhead ribozyme using luminescence spectroscopy, *Chem. Biol. 6*, 801−810.

22. Horrocks, W. D., Jr. (1982) Lanthanide probes of biomolecular structure, *Adv. Inorg. Chem. 4*, 201−261.

23. Horrocks, W. D. (1993) Luminescence spectroscopy, *Methods Enzymol. 226*, 495−538.

24. Holmquist, B. (1988) Elimination of Adventitious Metals, *Methods Enzymol. 158*, 6−12.

25. Dupureur, C. M., and Hallman, L. M. (1999) Effects of divalent metal ions on the activity and conformation of native and 3-fluorotyrosine-*Pvu*II endonucleases, *Eur. J. Biochem. 261*, 261−268.

26. Wagner, F. W. (1988) Preparation of metal-free enzymes, *Methods Enzymol. 158*, 21−32.

27. Muller, G., Kean, S. D., Parker, D., and Riehl, J. P. (2002) Temperature and pressure dependence of excitation spectra as a probe of the solution structure and equilibrium thermodynamics of a Eu(III) complex containing a modified dota ligand, *J. Phys. Chem. A 106*, 12349−12355.

28. *ITC Data Analysis in Origin* (1993), Microcal, Inc., Northampton, MD.

29. Martin, R. B., and Richardson, F. S. (1979) Lanthanides as probes for calcium in biological systems, *Q. Rev. Biophys. 12*, 181−209.

30. Brittain, H. G., Richardson, F. S., and Martin, R. B. (1976) Terbium(III) emission as a probe of calcium(II) binding sites in proteins, *J. Am. Chem. Soc. 98*, 8255−8260.

31. Spyridaki, A., Matzen, C., Lanio, T., Jeltsch, A., Simoncsits, A., Athanasiadis, A., Scheuring-Vanamee, E., Kokkinidis, M., and Pingoud, A. (2003) Structural and biochemical characterization of a new Mg^{2+} binding site near Tyr94 in the restriction enzyme *Pvu*II, *J. Mol. Biol 331*, 395−406.

32. Horton, J. R., and Cheng, X. (2000) *Pvu*II endonuclease contains two calcium ions in active sites, *J. Mol. Biol. 300*, 1049−1056.

33. Luk, C. K. (1971) Study of the nature of the metal-binding sites and estimate of the distance between the metal-binding sites in transferrin using trivalent lanthanide ions as fluorescent probes, *Biochemistry 10*, 2838−2843.

34. Wallace, R. W., Tallant, E. A., Dockter, M. E., and Cheung, W. Y. (1982) Calcium binding domains of calmodulin, *J. Biol. Chem. 257*, 1845−1854.

35. Shannon, R. D. (1976) Revised effective ionic radii and systematic studies of interatomic distances in halides and chalcogenides, *Acta Crystallogr. A32*, 751−767.

36. Matthews, B. W., and Weaver, L. H. (1974) Binding of lanthanide ions to thermolysin, *Biochemistry 13*, 1719−1725.

37. Chaudhuri, D., and Horrocks, W. D., Jr. (1997) Characterization of lanthanide ion binding to the EF-hand protein S100β by luminescence spectroscopy, *Biochemistry 36*, 9674−9680.

38. Reid, S. L., Parry, D., Liu, H.-H., and Connolly, B. A. (2001) Binding and recognition of GATATC target sequences by the *Eco*RV restriction endonuclease: a study using fluorescent oligonucleotides and fluorescence polarisation, *Biochemistry 40*, 2484−2494.

39. Conlan, L. H., and Dupureur, C. M. (2002) Multiple metal ions drive DNA association by *Pvu*II endonuclease, *Biochemistry 41*, 14848−14855.

40. Nastri, H. G., Evans, P. D., Walker, I. H., and Riggs, P. D. (1997) Catalytic and DNA binding properties of *Pvu*II restriction endonuclease mutants, *J. Biol. Chem. 272*, 25761−25767.

41. Cowan, J. A. (1995) *The Biological Chemistry of Magnesium*, VCH, New York.

42. Muller, G., Muller, F. C., and Riehl, J. P. (2004) On the use of high pressure to study the speciation, solvation, and excited-state energetics of luminescent lanthanide complexes, *J. Alloys Compd.*, in press.

43. Riehl, J. P., and Muller, G. (2004) Review of Circularly Polarized Luminescence Spectroscopy from Lanthanide Systems, in *Handbook on the Physics and Chemistry of Rare Earths* (Gschneidner, K., Bunzli, J.-C. G., and Pecharksy, V. K., Eds.) Vol. 34, Chapter 220, in press, Holland Publishing Company, Amsterdam.

44. Greenbaum, N. L., Mundoma, C., and Peterman, D. R. (2001) Probing of metal-binding domains of RNA hairpin loops by laser-induced lanthanide(III) luminescence, *Biochemistry 40*, 1124−1134.

45. Waddington, T. (1959) *Advances in Inorganic Chemistry and Radiochemistry*, Vol. 1, Academic Press, New York.

46. Bruno, J., Horrocks, W. D., Jr., and Beckingham, K. (1996) Characterization of Eu(III) binding to a series of calmodulin binding site mutants using laser-induced Eu(III) luminescence spectroscopy, *Biophys. Chem. 63*, 1−16.

47. Black, C. B., and Cowan, J. A. (1998) A critical evaluation of metal-promoted Klenow 3′-5′ exonuclease activity: calorimetric and kinetic analyses support a one-metal-ion mechanism, *J. Biol. Inorg. Chem. 3*, 292−299.

48. Brautigam, C. A., Aschheim, K., and Steitz, T. A. (1999) Structural elucidation of the binding and inhibitory properties of lanthanide (III) at the 3′-5′ exonucleolytic active site of the Klenow fragment, *Chem. Biol. 6*, 901−908.

49. Kay, J., Moore, J. W., and Glick, M. (1972) Structural studies of bridged lanthanide(III) complexes. Diaquotri(nicotinic acid)-holmium hexa(isothiocynanato)chromate(III) dihydrate and diaquotris(isonicotinato)lanthanum(III), *Inorg. Chem. 11*, 2818−2827.

50. Moore, J. W., Glick, M., and Baker, W., Jr. (1972) Crystal structures of hydrated lanthanide(III) nicotinates, La$_2$(C$_5$H$_4$NCO$_2$)$_6$-(H$_2$O)$_4$ and Sm$_2$(C$_5$H$_4$NCO$_2$)$_6$(H$_2$O)$_4$, *J. Am. Chem. Soc. 94*, 1858−1865.